Determination of the Sign of Nuclear Quadrupole Interaction by Laser-Radiofrequency Double-Resonance *

Tilo Blasberg and Dieter Suter
Institute of Quantum Electronics, ETH Hoenggerberg, CH-8093 Zürich

Z. Naturforsch. **49a,** 14–18 (1994); received August 8, 1993

We describe a new type of laser-radiofrequency double-resonance experiment, which allows to determine not only the absolute value but also the sign of nuclear quadrupole coupling constants. This determination of the sign, which is essential for the comparison with calculated EFG tensors, is not possible with purely magnetic experiments. The method has a high resolution and, because of the optical detection, also a high sensitivity. As an example, the quadrupole coupling constant for Pr^{3+}:$YAlO_3$ was measured at 4.38 K and was found to be negative.

Introduction

In 1935 Schüler and Schmidt, investigating optical spectra of rare earth elements, observed deviations from the Landé interval rule in the hyperfine structure. For an explanation of these deviations the authors postulated a hitherto unknown electrostatic coupling between the electronic charge and the quadrupole moment of the nucleus [1, 2]. With the development of NMR in condensed matter it became possible to study the quadrupole interaction of nuclei with their environment by a direct measurement of transition frequencies between different spin states. Two magnetic resonance methods are now frequently used to study the interaction of nuclear quadrupole moments in electric field gradients: nuclear magnetic resonance (NMR) in high magnetic fields and nuclear quadrupole resonance (NQR) in low fields. The electric field gradient is one of the most important signatures of the interaction of nuclear spins with their environement, and the measurement of nuclear quadrupole interactions serves as an important tool for the investigation of structure and dynamics in solid materials.

Both magnetic resonance methods, NMR and NQR, provide very precise absolute values of the coupling constants. However, they are insensitive to the sign of the quadrupole coupling as long as the high-temperature approximation is valid [3]. For typical values of quadrupole coupling constants it would therefore by necessary to cool the sample to a few mK to determine the sign by purely magnetic methods. Therefore in most cases only the absolute value can be determined and used for comparison with theoretically calculated electric field gradient tensors. Besides these direct methods, where photons with energies corresponding to the energy difference between nuclear spin states are absorbed, various nuclear methods are used, e.g. Mössbauer spectroscopy and perturbed angular correlation (PAC) [4], which use high energy photons in a high resolution experiment.

In this paper we discuss a new method, which uses optical and radiofrequency fields for the measurement of nuclear quadrupole interaction. This method has high precision and sensitivity and additionally allows the determination of the sign of the quadrupole coupling constants. The paper is structured as follows: in the following section we motivate the use of optical methods, as they allow in principle the determination of the sign of the quadrupole coupling constants. In practical systems with large inhomogeneous line broadening, double-resonance methods like spectral hole burning are required to resolve the nuclear quadrupole interaction. Unfortunately, in most of these experiments the sign information is lost. We then show how the additional use of a resonant radiofrequency field results in an experiment which yields directly the sign of nuclear quadrupole interaction.

Measurement of Nuclear Quadrupole Interaction by Laser Spectroscopy

In an idealized system without line broadening of the optical transitions the sign of the quadrupole cou-

---

* Presented at the XIIth International Symposium on Nuclear Quadrupole Resonance, Zürich, July 19–23, 1993.

Reprint requests to Tilo Blasberg, Institute of Quantum Electronics, ETH Hoenggerberg, CH-8093 Zürich.

0932-0784 / 94 / 0100-0014 $ 01.30/0. – Please order a reprint rather than making your own copy.

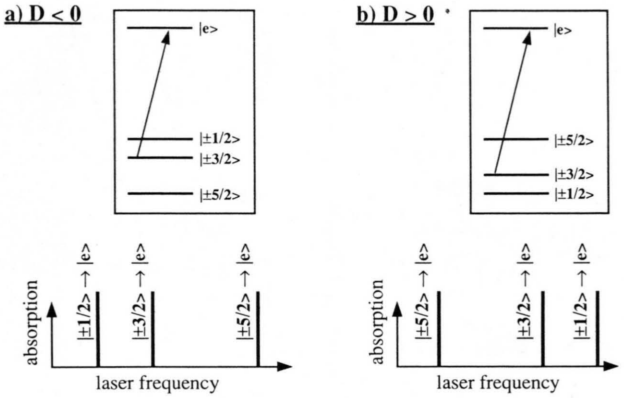

Fig. 1. Theoretical absorption spectra for the cases of negative (left) and positive (right) quadrupole coupling. The two insets show the energy level scheme for both case. |e⟩ represents an electronically excited state.

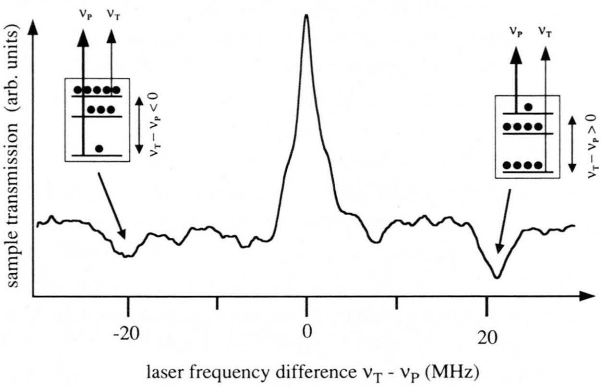

Fig. 2. Hole burning spectrum of Pr^{3+}:$YAlO_3$ at 3 K. The transmitted intensity is plotted as a function of the difference between the frequencies of the test and pump laser beams. The two insets explain, how optical pumping by the pump laser beam changes the sample transmission at positions where the laser frequency difference corresponds to the energy difference between two ground state sublevels.

pling can be determined from an optical absorption measurement. Figure 1 illustrates this experiment for a system with nuclear spin $I = 5/2$. For an axially symmetric environment the nuclear spin Hamiltonian can be written as

$$\mathscr{H}_Q = D(I_z^2 + (I(I+1)/3)\,, \qquad (1)$$

where the sign of the coupling constant D is to be determined. The eigenstates of this spin Hamiltonian are the I_z eigenstates with magnetic quantum numbers $\pm 5/2$, $\pm 3/2$, and $\pm 1/2$. In an optical absorption spectrum these states correspond to three distinct absorption lines, and the sign of the coupling corresponds to a given order of these three lines. The sign can be determined, because the symmetry of the magnetic interaction Hamiltonian is broken by coupling the spin system to the electronically excited state via an optical transition.

Obviously, the direct optical determination of the energies of the three spin states is only possible, if the frequency resolution is sufficient: the width of the optical resonance line must be smaller than the nuclear quadrupole interaction to be measured. Unfortunately, this is not the case in practice, since inhomogeneous line broadening mechanisms, e.g. due to crystal strain, exceed the size of the quadrupole interaction by several orders of magnitude.

In high resolution laser spectroscopy, various methods have been developed which overcome this limitation. One of these methods, spectral hole-burning, will be discussed in detail, as this method is an important part of the method to be presented.

In order to resolve the hyperfine interaction in systems with inhomogeneous line-broadening, spectral hole-burning uses two laser beams [5]. As shown in Fig. 2, an intense pump beam with frequency ν_P changes the populations of the three sublevels of the electronic ground state by optical pumping. If it is resonant with an optical transition from one sublevel to the excited state, it depletes the population of this sublevel and enhances the populations of the other non-resonant sublevels. A test laser beam measures the resulting absorption change of the sample. For the model system Pr^{3+}:$YAlO_3$ (Pr^{3+}:YAP) with $I = 5/2$, Fig. 2 shows this laser induced absorption change as a function of the frequency difference between the two laser beams. An absorption change is only observable if the test laser beam with frequency ν_T couples to one of the three sublevels of those atoms that were affected by the pump beam. Therefore signal contributions can only be expected at positions where the laser frequency difference $\nu_T - \nu_P$ corresponds to the energy difference between two resonant sublevels. Due to this double-resonance condition the frequency resolution in this experiment is significantly higher: it is only limited by the homogeneous linewidth of the nuclear spin transitions and the laser jitter.

As Fig. 2 shows, experimental hole-burning spectra are almost symmetric. The two insets show how this symmetry arises: both, the pump and the test laser beam, can couple to any of the three sublevels of the electronic ground state. Absorption changes are therefore observed for the same positive and negative frequency differences. An unambiguous sign determination from this spectrum is only possible if the efficiency of spectral hole burning varies significantly for the different allowed optical transitions and the relevant relaxation rates are known, so that the experimentally observed data can be compared with simulated spectra. Therefore only a few examples are reported where the sign of the quadrupole coupling constant could be derived from a hole burning spectrum [6].

This example showed that by increasing the frequency resolution in laser-spectroscopy, the sign information usually is lost. This is true for many other methods, including Raman heterodyne detection of NMR [7]. However, a combination of laser and magnetic resonance-spectroscopy allows the determination of all relevant parameters of the quadrupole interaction, including the sign of the coupling.

Raman Heterodyne Detection of NMR with two Laser Beams

Figure 3 uses a simplified level scheme to illustrate the principle of two beam Raman heterodyne detection of nuclear magnetic resonance. The levels labelled $|0\rangle$, $|1\rangle$, $|2\rangle$ are sublevels of the electronic ground state and $|e\rangle$ represents an electronically excited state (we neglect the quadrupole splitting of the electronically excited state). In the left hand diagram, Fig. 3a the pump laser, which is resonant with the transition between ground state sublevel $|0\rangle$ and the electronically excited state $|e\rangle$, redistributes the populations of the ground state sublevels through spectral hole-burning. Depending on the relaxation processes, it excites a population difference between, e.g., states $|1\rangle$ and $|2\rangle$. The radiofrequency (rf) field ω_{rf}, which is resonant with this transition, excites a coherent superposition of these two states. If the test laser field is resonant with the transition between one of the two levels and the excited state, this coherence is converted into an optical coherence by a coherent Raman process [7]. The frequency of the coherent Raman field is shifted by $\pm\omega_{\mathrm{rf}}$ relative to that of the test laser field. The Raman field propagates together with the test laser beam. On a photodetector, the two fields interfere, giving rise to a beat signal with frequency ω_{rf}. The amplitude of the component at the radiofrequency is

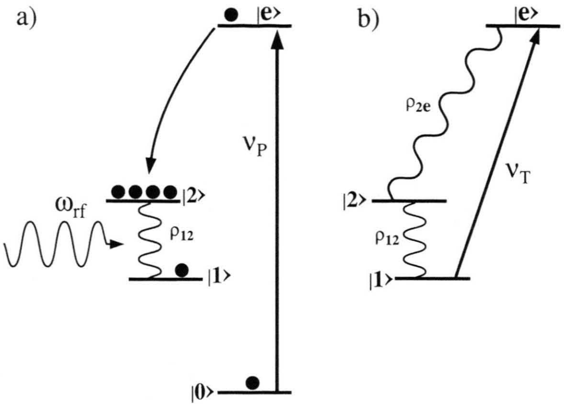

Fig. 3. Principle of two beam Raman heterodyne spectroscopy. States $|0\rangle$, $|1\rangle$, and $|2\rangle$ are sublevels of the electronic ground state, $|e\rangle$ represents an electronically excited state. a) The pump laser field modifies the ground state sublevel populations by spectral hole burning. The radiofrequency field excites a coherent superposition of the two unequally populated sublevels $|1\rangle$ and $|2\rangle$. b) The test laser field, interacting with the coherent superposition, creates a coherent Raman field in transition $|2\rangle \leftrightarrow |e\rangle$.

then

$$S_{\mathrm{rf}} \propto \mu_{12}\, \mu_{2\mathrm{e}}\, \mu_{\mathrm{e}1} (\varrho_{22}-\varrho_{11})\, |E_{\mathrm{T}}|^2\, B_{\mathrm{rf}}/(\gamma_{12}\, \gamma_{2\mathrm{e}}) \,. \quad (2)$$

As in the usual Raman heterodyne experiment with a single laser beam [7], the signal is therefore proportional to the product of the matrix elements of the three transitions involved, to the intensity of the test laser beam and to the rf amplitude. γ_{12} and $\gamma_{2\mathrm{e}}$ are the dephasing rates of the sublevel coherence and the optical coherence, $\varrho_{22}-\varrho_{11}$ is the population difference induced by spectral hole burning. In this experiment the frequency of the rf field is an additional parameter, which imposes a third resonance condition. As a result, a signal is observed only from those atoms which are optically pumped by the pump laser beam and for which the test laser is simultaneously resonant with a transition from levels 1 or 2 to the excited state. This contrasts with spectral hole burning, where signal contributions are obtained also when the test laser hits the transition from level 0 to the excited state.

Figure 4 shows, how this additional resonance condition reduces the symmetry of the spectrum and thus leads to distinguishable spectra for the two possible signs of the quadrupole coupling constant D. The stick spectra at the top indicate qualitatively the expected Raman heterodyne signal amplitude as a function of the *difference* $\nu_{\mathrm{T}}-\nu_{\mathrm{P}}$ between the frequency ν_{T} of the test laser beam and the frequency ν_{P} of the pump laser beam. With the rf field we select a transition between

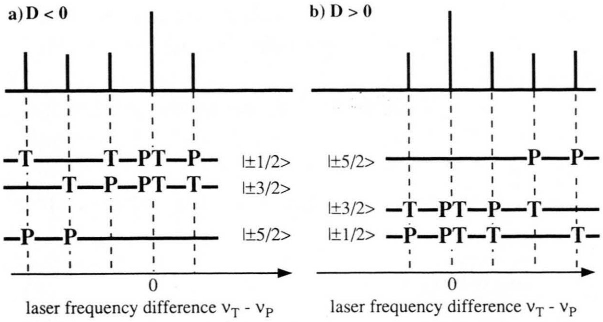

Fig. 4. Theoretical spectra of the Raman heterodyne signal as a function of the laser frequency difference for negative (left) and positive (right) quadrupole coupling. For each resonance line, the letters indicate the spin substates that are coupled to the excited state |e⟩ by the pump (P) and test (T) laser beam.

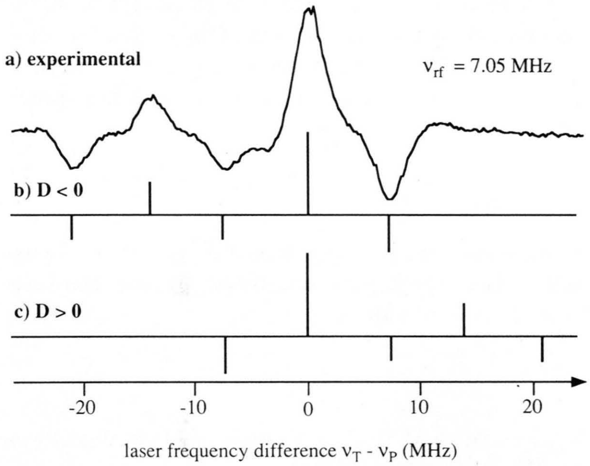

Figure 5. Experimental spectrum (a) of the Raman heterodyne signal as a function of the frequency difference between test and pump laser beam. The theoretical stick spectra (from Fig. 4) indicate the line positions for negative (b) and positive (c) quadrupole coupling. The rf frequency was in resonance with the $\pm 1/2 \leftrightarrow \pm 3/2$ transition of the electronic ground state.

two ground state sublevels (in our experiment the $m_I = 1/2$ and $m_I = 3/2$ states); only those atoms contribute to the observed signal, for which the test laser beam is resonant with a transition from one of these states to an excited state. With two electronic transitions to which the test laser beam can couple, and three transitions that can be excited by the pump laser beam, we expect a total of six signal components. In the lower part of Fig. 4 the letters P and T indicate the ground state sublevels that are simultaneously in resonance with the two laser beams for the given frequency difference. In two cases pump and test frequencies coincide, while the four other cases occur at clearly distinct frequency differences. The comparison between the two cases of opposite sign shows that the reversal of the sign of the quadrupole coupling leads directly to an inversion of the spectrum.

In our experiment we used Pr^{3+}-ions [8] substituted in a $YAlO_3$ (YAP) crystal matrix at the Y lattice sites in a concentration of 0.1%. The crystal of size $5 \times 5 \times 1$ mm was cooled to 4.38 K in an He flow cryostat and the two laser beams propagated along the crystal *c* axis. The laser frequency was resonant with the transition between the $^3H_4$ ground state and the $^1D_2$ excited state ($\lambda = 610.6$ nm). The frequencies of pump and test laser beam, which were derived from the same ring dye laser, were shifted independently with two acousto-optic modulators. The difference between the two laser frequencies was determined by the rf synthesizers, independent of the laser jitter. A third rf synthesizer was set to 7.05 MHz, selecting the $|\pm 1/2\rangle \leftrightarrow |\pm 3/2\rangle$ transition. The rf signal was amplified to 3 W and applied to the crystal by a rf-coil that was part of a tuned circuit. The resulting rf field of 10 μT was oriented perpendicular to the X principal axis of the nuclear quadrupole tensor, along the crystal *a*-axis.

Figure 5 shows the observed amplitude of the Raman signal as a function of the difference between the two laser frequencies. The width of the optical resonance lines is dominated by the (unresolved) nuclear quadrupole splitting of the electronically excited state and the laser frequency jitter. The stick spectra, which show the expected line positions, are taken from Fig. 4. As expected, the observed spectrum is asymmetric with respect to the sign of the laser frequency difference. The observed resonance lines at -14 MHz and -21 MHz and the absence of lines at $+14$ MHz and $+21$ MHz agrees well with the spectrum expected for $D < 0$ and is clearly incompatible with $D > 0$.

For a determination of the absolute value of the coupling constants we scanned the radiofrequency over the magnetic resonance with the laser frequency difference kept constant at $\nu_T - \nu_P = 0$. In zero magnetic field the Raman heterodyne signal vanishes due to interference between the degenerate transitions [9]. Therefore we used a magnetic field to remove this degeneracy. Figure 6 shows the amplitude of the observed Raman heterodyne signal as a function of the radiofrequency. The magnetic field of 41.4 G was ori-

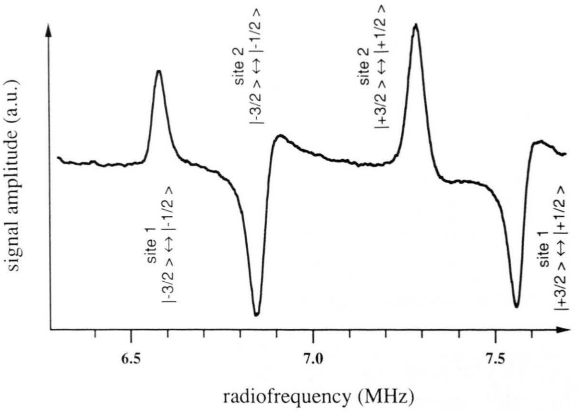

Fig. 6. Amplitude of the Raman heterodyne signal as a function of the radiofrequency for the constant laser frequency difference $\nu_T - \nu_P = 0$. An external magnetic field was applied to lift the sublevel degeneracy. The magnetic field causes different splittings for the two non-equivalent sites in the crystal.

ented in the YZ-plane, the rf-field was oriented along the X principal axis of the quadrupole tensor and the temperature of the sample was 3.12 K. Because an rf-field is used to excite the coherence between two ground state sublevels, the spectrum has the same high frequency resolution as conventional magnetic resonance experiments. In the spectrum four resonances can be observed corresponding to transitions between Zeeman-split sublevels of two non-equivalent sites in the crystal. From the observed line positions we extrapolated the transition frequencies in zero magnetic field.

At a temperature of 3.12 K we measured the frequencies 7.074 MHz for the $|\pm 1/2\rangle \leftrightarrow |\pm 3/2\rangle$ transition and 14.126 MHz for the $|\pm 3/2\rangle \leftrightarrow |\pm 5/2\rangle$ transition. These data were fitted to the nuclear spin Hamiltonian.

$$\mathscr{H}_Q = D(I_z^2 + I(I+1)/3) + E(I_x^2 - I_y^2)\,. \qquad (3)$$

From the data we conclude that $D = -3.5324$ MHz and $\eta = |3E/D| = 0.035$.

In the experiment the time for the rf-sweep was 1 s and the signal of Fig. 6 was averaged 10 times. Under the experimental conditions the total number of Pr-ions contributing to the Raman signal is approximately 10^{11}.

In conclusion, we have demonstrated that both, the coupling constants and the sign of the nuclear quadrupole interaction can be determined in a laser-radiofrequency double-resonance experiment with high precision and high sensitivity.

Acknowledgement

We would like to thank R. Kind for helpful discussions. This work was supported by the Schweizerischer Nationalfonds.

[1] H. Schüler, and Th. Schmidt, Z. Physik **94,** 457 (1935).
[2] For a historical overview see P. Brix, Z. Naturforsch. **41 a,** (1986).
[3] A. Abragam, The Principles of Nuclear Magnetism, Oxford University Press, Oxford 1961.
[4] H. Haas, Z. Naturforsch. **41 a,** 78 (1986).
[5] S. Voelker, Ann. Rev. Phys. Chem. **40,** 499 (1989).
[6] K. Holliday, M. Croci, E. Vauthey, and U. P. Wild, Phys, Rev. B **47,** 14741 (1993).
[7] N. C. Wong, E. S. Kintzer, J. Mlynek, R. G. DeVoe, and R. G. Brewer, Phys. Rev. B **28,** 4993 (1983).
[8] T. Blasberg, and D. Suter, submitted to Phys. Rev. B.
[9] M. Mitsunaga, E. S. Kintzer, and R. G. Brewer, Phys. Rev. B **31,** 6947 (1984).